Chapter 1

Introduction

1.1 Quantum information science

Quantum information science is the part of information science that includes the possibility for information to behave quantum mechanically. Specifically, in digital format, classical information stored in a single bit can have the value 0 or 1. For the quantum case, the state of a bit (in that case named *qubit*) can be 0 and 1 at the same time, according to a quantum state $|\Psi\rangle = \alpha\,|0\rangle + \beta\,|1\rangle$. Here $|0\rangle$ and $|1\rangle$ represent two orthogonal quantum mechanical states (and α and β are the probability amplitudes for a superposition state), which can for example be the spin-up and spin-down state of an electron, or two orthogonal polarization states of a photon. In addition, the quantum state of a system with many qubits can contain correlations between qubits (which are then said to be *entangled*) that have no classical analogue [1, 2].

As a research field, quantum information science has seen a strong development [3, 4, 5] since a few discoveries that showed that quantum information processing can perform significantly better than classical information processing. In 1984, Bennett and Brassard discovered the first of several protocols that enable complete protection of communication against eavesdropping [6, 7]. In 1997, Shor and Grover reported algorithms that can speed up certain computational and data-search tasks by many orders of magnitude [8, 9]. However, practical realization and widespread application in society is still under development. The field is showing steady progress, but realizing a large-scale quantum-information system remains challenging. This is mainly because noise from any environment around the qubits rapidly disturbs their quantum state, in particular for systems where one can also accurately and rapidly control the quantum states. Research has thus been focussed on developing qubits that show a good trade-off

between having long-lived quantum states and possibility of control. Quantum information systems with a few qubits have been realized, but scaling these up to many-qubit systems is even more challenging, and this is currently one of the main research topics in this field [3, 4, 5].

1.2 Goals and scope of this PhD research

The need for this scalability directed research to realizing qubits in solid state, with the prospect to build on technology and expertise from the semiconductor industry [10, 11]. The research presented in this PhD thesis is part of this development. Rather than directly investigating quantum information functionalities, the research had as goal to develop fundamental knowledge about the possibilities and limitations that come forward when implementing qubits in solid state. High-level control over quantum systems (including light-matter interactions) was initially mainly demonstrated in the fields of atomic physics, laser physics, and quantum optics. The research in this thesis explores similar laser control over systems in solid state, with optically-active systems inside a semiconductor material that have strong similarity with isolated atoms.

The potential relevance for quantum information science is mainly for quantum communication [6, 7]. Here, for many proposals, optical pulses (often called flying qubits) are used to transfer the information, since they travel with the speed of light and interact weakly with their surrounding. However, for high-level performance of such systems, a quantum communication network needs memory nodes that can store quantum information on long-lived states in matter, such as electronic or nuclear spin states [12, 13, 14]. To realize this, one needs to address the challenge to transfer the quantum information contained in an optical pulse onto a spin state, and to transfer it back from the spin onto a next optical pulse when needed [15]. Such dynamics was already widely studied with systems from atomic physics [16, 17, 18]. This PhD research explored whether it can also be implemented with spins in solid state.

The work thereby addresses two main challenges. First, the need for having optically-active material with spin degrees of freedom that have a very long coherence time. Second, the need for having such a material with spins that can also give a very strong interaction between spins and optical pulses. In several experiments strong coupling is realized by placing the material in a high-finesse optical cavity. However, it is technologically very demanding to fabricate and tune such cavities [19, 20, 21]. This thesis has relevance for an alternative ap-

proach, where the strong coupling is realized by working with an ensemble of (ideally) identical qubit systems, that together act as one functional qubit and together form a medium with high optical density. Earlier proposals showed that this provides a route to very robust quantum-optical control schemes that can be applied for preparing non-local entanglement between spins, quantum communication, and functions that use strong optical non-linearities [12, 16, 17, 18]. A critical step toward implementing these schemes is the realization of Electromagnetically Induced Transparency (EIT, see below).

For these studies, our material system of choice was the silicon (Si) donor center in the semiconductor gallium arsenide (GaAs), in its neutral charge state. This systems is called the D^0 system [22], and behaves as an artificial hydrogen atom (or any other alkali atom) in solid state: it has a single donor electron that is in orbit (localized) around the donor impurity atom, and it has optical transitions to excited states that can be addressed with laser fields (with photon energies that are less than the band gap of GaAs). Via the polarization of the laser fields, or by applying magnetic fields, one can selectively address the spin states of the D^0 electron. The rational to work with this material system is that GaAs material can be grown as an ultra-clean single crystal, with a low concentration of Si donor impurities. Further, the physics of semiconductor optics with GaAs has already been studied for decades, as well as the related semiconductor device technology. This together makes GaAs one of the best available material systems for studies of optically controlling quantum states in matter, and quantum-optical interactions with these states.

With this material system, this PhD research investigated laser control of an ensemble of D^0 systems. This has a strong analogy with addressing a vapor of alkali atoms, but the differences with the solid-state version bring some interesting advantages and open questions. A first advantage is that the D^0 systems are at fixed positions in the solid, while experiments that address a vapor of alkali atoms suffer from atoms drifting out of the control volume. Further, the GaAs version can easily be implemented in micrometer-scale GaAs structures, while atomic vapors need control systems (vacuum spaces) that are large and difficult to operate. However, operating such an atom-like ensemble in solid state possibly also brings new limitations for using them as qubits, and open questions on the physics that governs their behavior. This thesis addresses four topics for this line of research.

1) (*Chapter 2*) The realization and study of *Electromagnetically Induced Transparency* (EIT) with a D^0 ensemble. EIT is a two-laser control technique where two lasers together (both with high photon energies) can control the quantum state of an electron spin (with two states at much lower energies that can have long-lived quantum coherence). EIT is a fundamental effect that underlies many quantum-enhanced functionalities that use both long-lived spin states and optical signals, and has been widely studied with alkali-atom vapors [18]. EIT can also give extreme non-linearity for an optical medium, and a dynamical form of EIT can be operated as a storage technique for optical pulses [16, 17, 18]. Chapter 2 reports the first realization of EIT with a semiconductor, and several aspects that limit the quality of EIT with GaAs D^0 systems.

2) (*Chapter 3*) A spectroscopic study of the optically-excited state manifold of the D^0 system. While earlier work already described the structure of the D^0 excited state, our EIT experiments showed that identifying these levels in EIT experiments is nontrivial and requires new spectroscopic studies. In addition, better understanding of these levels, and the optical transitions to these levels, is essential for optimizing EIT-type control of GaAs D^0 systems.

3) (*Chapter 4*) Developing how EIT can be used as a tool for controlling and detecting interactions between D^0 electron spins and the nuclear spins of Ga and As atoms in their direct vicinity. In an alkali atom, the active outer electron has hyperfine interaction with one nuclear spin. However, the orbital cloud of the D^0 electron in GaAs has a radius that is about a factor 20 larger, and it thus covers many GaAs lattice sites. All Ga and As atoms have nonzero nuclear spins. Consequently, each D^0 electron spin has hyperfine interaction with about 10^5 nuclear spins. Understanding the physics of these interactions is essential for optimal application of D^0 electron-spin states. This chapter reports how EIT can be used to control and study these hyperfine interactions.

4) (*Chapters 5 and 6*) The studies of EIT effects in micrometer-scale GaAs structures required new dedicated experimental setups and instruments. Chapters 5 and 6 report on the development and testing of these experimental setups and instruments.

The remainder of this first chapter provides a further introduction to the research field and the contents of this PhD thesis.

1.3 The D^0 system in GaAs

1.3.1 Bulk GaAs and the D^0 system

This section provides a further introduction into the properties of the D^0 system in GaAs, as formed by Si donor atoms at low concentration. In that case, for the material at temperatures below about 10 K, and without background light, the Si donors will not be ionized, and thus form centers where single excess (donor) electrons are localized in the GaAs host. Further, the Si atoms fit in the GaAs lattice, all in the same way, replacing Ga atoms. Consequently, when the GaAs host is a single crystal and kept strain free in further processing, the quantum systems formed by the Si D^0 systems all have nearly identical properties: as compared to many other optically-active centers in solid state such a D^0 ensemble is typically very homogeneous for properties like its energy-level spacings.

High-quality and high-purity GaAs crystals with a low concentration of intentional Si doping can be grown with molecular-beam epitaxy (MBE) techniques. For the research in this thesis we uniquely worked with MBE-grown material from the group of A. D. Wieck and D. Reuter at the Ruhr University Bochum, Germany. In our materials, the concentration of Si donors was typically around 3×10^{13} cm^{-3}, which corresponds to an average distance of about 180 nm between the Si donors (while the D^0 electron orbit has a radius of about 10 nm). A background of other impurity atoms had a total concentration that was about a factor 100 lower, and mainly carbon.

GaAs is a semiconductor with a direct band gap, meaning that it has strong optical transitions for excitations from the top of the valence band to the bottom of the conduction band. For such optical transitions across the gap, there are clear selection rules that correlate the polarization of optical fields to the spin of charge carriers involved in the transition [22, 23]. Already several decades ago it was studied how this can be used for optical orientation of electron spins in bulk GaAs, and how this can in turn also polarize nuclear spins [24]. More recently, with pump-probe (preparation-detection) pulsed-laser control, time-resolved studies of these effects showed that spin coherence of free conduction-band electrons can have dephasing times in excess of 100 ns [25]. Besides the photo-excitation of free charge carriers, optical excitation can lead to the formation of excitons (hydrogen-atom-like bound electron-hole pairs). For the exciton in its lowest energy state, this is an excitation with an energy of the bulk band gap (1.519 eV at low temperatures) minus the exciton binding energy (4.2 meV) [23]. These

optical properties for bulk GaAs will still play a role for the localized D^0 systems, with optical transitions just inside the bulk GaAs band gap.

The D^0 system is a shallow donor. When not ionized and with the donor electron in its ground state, the electron is in a localized state with an energy that is 5.8 meV below the bottom of the conduction band. This is the binding energy of the donor electron to the Si core ion. The bound states of this hydrogen-like system are well described with effective-mass theory [22], using the time-independent Schrödinger equation

$$\Big(-\frac{\hbar^2 \bigtriangledown^2}{2m_e^*} - \frac{e^2}{4\pi\epsilon_0\epsilon_r r}\Big) F_n(\overrightarrow{r}) = E_n F_n(\overrightarrow{r}), \tag{1.1}$$

for describing the envelope wave function $F_n(\overrightarrow{r})$ and energies E_n. Here m_e^* is the effective mass of the electron in GaAs (0.067 m_e, where m_e is the free electron mass). Further, e is the electronic charge, ϵ_0 is the permittivity of the free space, ϵ_r is the relative permittivity for GaAs (12.56), and n labels the quantum number. The quantized energies E_n have values (with respect to the bottom of the conduction band) that can be expressed as

$$E_n = -\frac{m_e^*}{m_e}\frac{1}{\epsilon_r^2}\frac{R_H}{n^2}. \tag{1.2}$$

Here R_H is the Rydberg constant for the hydrogen atom (13.6 eV). This yields the 5.8 meV binding energy for the system in its $n = 1$ ground state. For the ground state $F_n(\overrightarrow{r})$ has a form similar to the $1s$ ground state of hydrogen (Fig. 1.1). However, its Bohr radius is significantly larger (a_0 = 9.9 nm) due to the low value for the effective mass and the high value for the relative permittivity. This justifies the effective-mass approach. Note that for the full wave function of the D^0 electron $F_n(\overrightarrow{r})$ must be multiplied with a Bloch function, which then describes the structure in the wave function at the scale of the lattice periodicity (lattice constant is 0.565 nm) [23].

1.3.2 D^0-D^0X optical transitions

For optical control and probing of the D^0 system we will consider excitations to a state where an additional exciton (X) is bound to the D^0 system, see Fig. 1.1. This excited system is denoted as D^0X, often called the (neutral) donor-bound exciton, but sometimes also referred to as a bound trion system (Fig. 1.1). This D^0X system can thus be seen as an atom with three interacting charge carriers, but analyzing its energy eigenstates is much more complex due to the solid-state

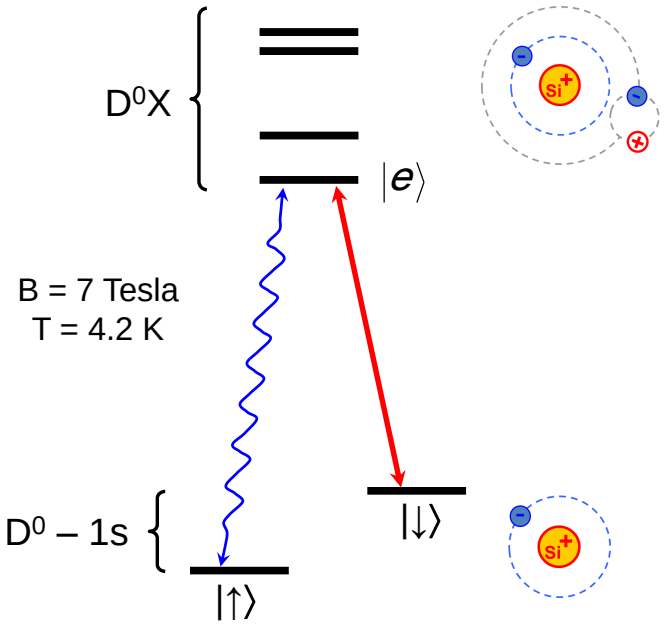

Figure 1.1: Level scheme (left) and cartoon representations (right) of the D^0 and D^0X energy eigenstates in a magnetic field of 7 T. For the D^0 ground state we only consider the lowest-energy orbital state ($1s$ envelope wave function). The D^0-$1s$ state has two energy levels, the Zeeman-split states spin-up $|\uparrow\rangle$ and spin-down $|\downarrow\rangle$ for the localized electron. The optically excited states are a series of levels for the D^0X complex, which has an additional electron-hole pair (exciton, X) bound at the D^0 site. With two electrons and one hole in a three-body bound state around the Si core ion, these D^0X states are also referred to as trion states. The arrows in the level scheme represent laser fields that drive transitions between the levels, selectively addressing the D^0 spin states and one level $|e\rangle$ of the D^0X complex.

environment. This D^0X system was extensively studied before, both in theory and in experiment. Part of this work identified valid approximations for the description, and it showed good agreement between experiment and a theoretical framework for analysis. Still, the complexity of the system is too high for a general theoretical description (either analytical or numerical) that cover all aspects (such as magnetic field dependence). New investigations in this area are presented in Chapter 3.

The D^0X system has many energy eigenstates. In a magnetic field of about 7 T, the lowest levels appear as well-separated lines in spectroscopy (typically at least 6 lines can be observed). The splittings correspond to typical values for electronic Zeeman splittings. For an order of magnitude of the energies, we consider here further the case of zero magnetic field. The energy of a D^0-D^0X

transition (assuming lowest energy eigenstate for both) is then the GaAs band gap, minus the free-exciton binding energy, minus the binding energy of the exciton to the D^0 system (and a further small correction from interactions and re-arrangement of the three charge carriers). These are all terms at the few meV scale, and experimentally the spectral line of the D^0-D^0X transition appears 0.9 meV lower in energy than the transition for creating $n = 1$ free excitons, at an energy of $\sim(4.2 + 0.9) = 5.1$ meV below the band gap [23] (see Fig. 2.1(a)). The wavelength difference for the $X_{n=1}$ and D^0-D^0X transition thus corresponds to $\triangle\lambda = 55$ Å, with the central wavelength for D^0-D^0X at ∼8188 Å (small shifts are observed due to strain). In an applied magnetic field of $B = 7$ T, the Zeeman splitting $E_Z = g\mu_B B$ for the D^0 electron is 0.166 meV, which corresponds to a shift in wavelength of about 0.9 Å (where the D^0 g-factor is $g = -0.42$ [26, 27], and μ_B is the Bohr magneton).

1.3.3 Lambda system

For getting EIT-type control, the D^0-D^0X must be operated as a *lambda system* (a three-level scheme that resembles the Greek letter Λ, see Figs. 1.1, 1.3). This is realized by applying a field of about 7 T to the GaAs material, which Zeeman splits the two spin states $|\uparrow\rangle$ and $|\downarrow\rangle$ of the D^0-1s system (Fig. 1.1). These two spin states both have dipole-allowed optical transitions to the D^0X complex, and often both to the same level $|e\rangle$ of this complex. For realizing a lambda-type control scheme, we tune two lasers such that each drive a transition from one of the states $|\uparrow\rangle$ and $|\downarrow\rangle$ to the same level $|e\rangle$ (we mostly work with one of the lowest levels $|e\rangle$ of D^0X, Fig. 1.1). Most of the lowest optical transitions only couple to laser fields with a particular polarization (Chapter 2).

1.3.4 Experimental considerations and setup

Before further describing the EIT control scheme that we aim to investigate with D^0 ensembles, we use the properties described till now for listing the implications for experimental work on this system. First, the requirement to avoid ionization of a significant fraction of the D^0 systems and (since our experiments use the excited states) D^0X systems gives in practice that the temperature should be well below 10 K. This is most conveniently implemented by doing all experiments in a helium bath cryostat (4.2 K sample temperature). This also allows for using superconducting magnets for applying tunable fields of about 7 T in the sample volume. These two aspects together compromise the ease of optical access: the

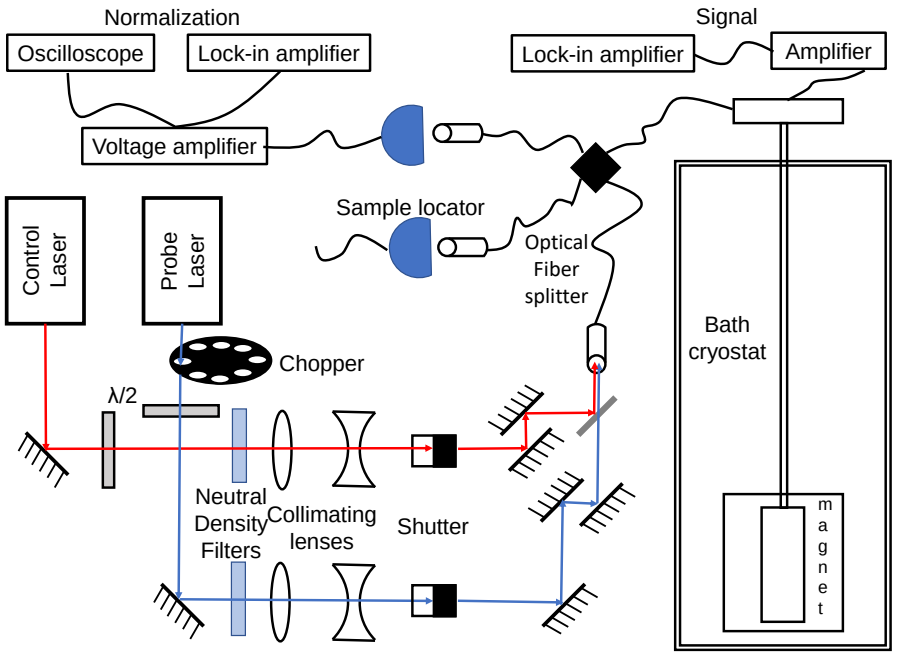

Figure 1.2: Schematic of the the experimental setup, see main text for details. Further details and a photograph of parts inside the bath cryostat are presented in Fig. 5.1.

sample volume is deep inside a cryostat, and it is limited in size due to the surrounding magnetic coil (a cylinder of 50 mm diameter, see Fig. 5.1). Still, it is needed to deliver and extract optical fields to this sample volume with well-defined optical polarizations and beam profiles.

For this approach, we build a dedicated experimental setup where laser fields reach the sample volume via polarization maintaining fibers, while light could also be coupled out of the measurement volume via fibers (see Fig. 1.2, more detailed descriptions are presented in Chapters 5 and 6). In the sample volume, for a typical experiment, we mounted small lenses and a transparent heat-sinked sapphire working surface, on which we adhered a 10 μm-thick GaAs layer (simply using Van der Waals adhesion, as an approach to get low strain in the GaAs layer from its mounting). This allowed for optical transmission experiments with the GaAs layer. Compact piezo motors in the sample volume were applied for focussing the laser fields to micrometer-scale spots (see Fig. 5.1), and allow for focussing on different areas of the GaAs layer.

Figure 1.2 presents the overall experimental setup in one of its typical forms. Several aspects were varied or improved during the course of the research, and this will be specified along with specific results in the chapters of this PhD thesis. Essential instruments and functionalities in the schematic of Fig. 1.2 are as

follows. Two tunable lasers with 75 kHz linewidth with 50 GHz mode-hop-free scanning capability (optimized for use around 820 nm wavelength) provided the optical fields. Half-wave-plates were used in the laser path to define linear polarizations. A chopper was used to modulate the scanning probe laser (but for part of the measurements we used the chopper in the beam of the fixed control laser). Collimating lenses were used to shape the beam and minimize its divergence. The laser light was steered into the fiber-optic-coupler using mirrors and beam splitters. A polarization-maintaining optical-fiber beam splitter was used. It has three channels excluding the input channel. One channel was used to connect another polarization-maintaining optical fiber to steer light into the bath cryostat. Inside the cryostat, light falls on the sample and transmitted light was detected using a photodiode in the sample volume (or steered to detectors outside the cryostat via additional optical fibers). The signal from the photodiode was amplified and detected using a lock-in amplifier. The second channel of the optical-fiber beam splitter was used as a normalization channel. The normalization channel was coupled to a photodiode with amplifier and was further connected to an oscilloscope and lock-in amplifier. The third channel could be used to detect reflection from the sample. This was only used for locating and positioning the sample inside the cryostat.

1.4 Electromagnetically induced transparency

Electromagnetically induced transparency (EIT) is the phenomenon that an absorbing optical transition becomes transparent for a probe-laser field because destructive quantum interference in the dynamics of a quantum system prohibits populating the optically excited state. The destructive quantum interference can occur because two laser fields (the probe laser field, and a control laser field) both drive optical transitions. EIT can occur with three-level systems as in Fig. 1.3(a), for which it is essential that the two low-energy spin states can have a long-lived quantum coherence and that one can selectively address the two optical transitions. In Fig. 1.3(a) this is depicted for the Zeeman-split spin states of the D^0 system and one of the lowest states $|e\rangle$ of the D^0X complex.

A homogeneous ensemble of these systems can become transparent for the probe laser when it meets the condition for two-photon Raman resonance with the applied control laser (the difference in laser photon energy exactly matches the energy splitting between $|\uparrow\rangle$ and $|\downarrow\rangle$). Under these conditions the systems are trapped in a dark state, which is in the case of ideal spin coherence the quantum

superposition state

$$|\Psi_{dark}\rangle = \frac{\Omega_c |\uparrow\rangle - \Omega_p |\downarrow\rangle}{\sqrt{|\Omega_c|^2 + |\Omega_p|^2}}, \tag{1.3}$$

where Ω_c (control) and Ω_p (probe) are the Rabi transition frequencies associated with the driven optical transitions [18, 28]. The phenomenon is closely related to Coherent Population Trapping (CPT). CPT only concerns the trapping in a dark state upon two-laser driving. EIT concerns the optical transmission properties of a medium with identical systems in, or nearly in, a CPT state. Notably, the requirement for homogeneity of energy splittings mainly concerns the ground-state spin splitting, since the two-photon resonance condition is insensitive to shifts of the energy of state $|e\rangle$. Indeed, CPT and EIT are robust against a moderate amount of inhomogeneity for the energy of state $|e\rangle$ (strong inhomogeneity can still comprise EIT when it becomes very much larger than the homogeneous line width of transitions to $|e\rangle$, or when the energy shifts become as large the splitting between $|e\rangle$ and other excited-state levels [18]). This makes EIT-based control schemes robust against a range of technical and material imperfections.

The experimental fingerprint of EIT is shown in Fig. 1.3(b,c). For the description here we assume that fully on resonance the medium has an optical thickness of about 3 (significant absorption, but no strong influence yet on the line width of spectral lines). With only the probe laser on, and frequency scanning it across the $|\uparrow\rangle$-$|e\rangle$ resonance, the transmission spectrum show a single dip (assuming that the probe laser is weak enough to avoid complete optical pumping into the state $|\downarrow\rangle$, as balanced by spin relaxation). The line width corresponds to the dephasing rate for the state $|e\rangle$ (when not significantly power broadened by the laser).

Now assume that both the probe and the control laser are on, and tuned to photon energies near two-photon resonance. When the probe scan passes the detuning of exact two-photon resonance, the lambda systems get trapped in the dark state, and no longer absorb the laser fields. Hence, the medium becomes transparent, which appears in the spectrum as a narrow EIT peak inside the absorption dip. For strong enough control laser and a long spin dephasing time, the transmission is fully restored to unity. The EIT line width can be as narrow as the spin dephasing rate (when not significantly power broadened by the lasers). The spectra in Fig. 1.3(b,c) are calculated with standard EIT theory [18], with parameters that are typical for the D^0 system (further discussed in Chapter 2).

For the case of a finite spin dephasing time (in the sense of an inhomogeneous dephasing time T_2^* for a spin ensemble), the EIT peak only develops when the control laser is of high enough intensity: the cycling between the ground state

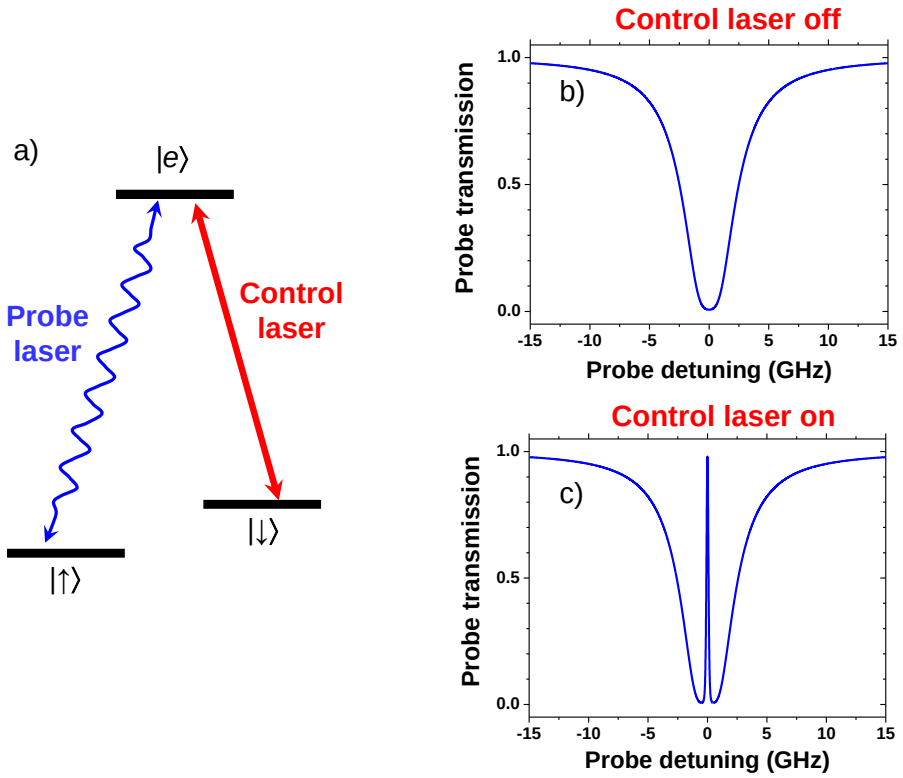

Figure 1.3: **(a)** Lambda energy-level scheme with a probe and control laser coupled to the system in a manner that can drive EIT. **(b)** Probe-laser transmission spectrum for the case that the control laser is off (weak probe laser, no complete optical pumping). In that case, the transmission spectrum shows a dip that corresponds to resonance with the $|\uparrow\rangle$-$|e\rangle$ transition. **(c)** Probe-laser transmission spectrum for the case that the EIT control laser is on. In this case, the transmission spectrum shows a sharp peak (the EIT transmission peak) inside the absorption dip of panel (b). The probe frequency scan is referenced with respect to the condition for two-photon resonance (see main text).

and excited state should be fast enough to experience the quantum coherence contained in the superposition of the two spin states, such that the destructive quantum interference in the dynamics can play a role. When assuming that the control laser has a higher intensity than the probe laser ($\Omega_c > \Omega_p$), the condition for getting EIT is (accurate for optical thickness $\lessapprox 1$)

$$|\Omega_c| > \sqrt{\gamma_e \, \gamma_{\uparrow\downarrow}}, \tag{1.4}$$

where γ_e and $\gamma_{\uparrow\downarrow}$ are, respectively, the excited-state and spin dephasing rate [18].

For these same conditions, the width of the EIT peak is approximately [18]

$$\triangle_{EIT} \approx \sqrt{\gamma_{\uparrow\downarrow}^2 + |\Omega_c|^2}. \tag{1.5}$$

For systems with slow spin dephasing, EIT can give a very significant yet extremely sharp spectral feature, which is a controllable optical non-linearity: the sharpness of the feature can be controlled via Ω_c. This provides the basis for strong interaction between optical pulses and spin states. More in general, it is a path for controlling absorption and refraction of the medium.

At the start of this PhD research, EIT was most extensively studied with ensembles of alkali atoms. A key result from this field was that it established that EIT gives access to very robust quantum optical techniques for controlling strong correlations between the quantum state of a collective spin excitation in an ensemble and the state of the probe field [12, 16, 17, 18]. Such experiments are technically less demanding than similar quantum optical experiments that use a single atom in a high-finesse optical cavity [19, 20, 21]. In particular, this field realized studies of quantum entanglement between atomic ensembles with several meters spatial separation, with state preparation and readout via a quantum optical measurement scheme [29, 30]. Notably, this was realized only a few years after initial work on EIT applications demonstrated slow light (down to $\sim$17 m/s) [31] and storage of light [32]. The work in this PhD research investigated initial steps for light storage and studies of nonlocal quantum entanglement with spins in solid state [28, 33].

1.5 Nuclear environment and dynamic nuclear polarization

The previous section discussed that high-quality EIT needs a spin ensemble with a long dephasing time. For the D^0 electrons in GaAs the spin dephasing in mainly due to hyperfine interactions between each D^0 electron and about 2×10^5 nuclear spins within the D^0 electron cloud (all stable Ga and As isotopes have non-zero nuclear spin). When the magnetic field is below 20 T and the temperature above a few mK, the state of such a nuclear spin ensemble is that the spins have almost fully randomized orientations at thermal equilibrium. That is, for the thermal-equilibrium conditions as in our experiments the average nuclear spin polarization is very close to zero in all directions. However, when randomly orienting N nuclear spins, there will be statistical fluctuations around zero polarization with

a magnitude of $\sqrt{N}$. Hence, each D^0 spin will experience hyperfine interaction with a small non-zero nuclear spin polarization, that has a random value in the range of $\pm\sqrt{N}$ oriented nuclear spins. Via the hyperfine interaction this acts as an effective magnetic field (called Overhauser field) on the D^0 spin [34, 35], with a random value in the range ± 15 mT. This results in the spin dephasing time $T_2^* \approx 2$ ns for a D^0 ensemble. Notably, when removing this mechanism the spin dephasing times will be in excess of 7 μs, as demonstrated with optically-controlled spin-echo experiments [36].

Consequently, the T_2^* value for a D^0 ensemble can be made longer if the nuclear spins can be driven into a more ordered state. A path to such control can be based on using Dynamic Nuclear Polarization (DNP). DNP is the phenomenon that a nuclear spin ensemble can get polarized due to hyperfine interaction with an electron spin that is driven away from it thermal-equilibrium polarization. When (in part) the electron spin polarization relaxes via hyperfine interaction with the nuclear spins, the polarization of the electron spin will be transferred onto the nuclear spin ensemble. In its most basic form, such a relaxation process is a electron-nuclear spin flip-flop process, where angular momentum is conserved [34]. However, the full dynamics of DNP can be much more complex, with a role for energy and/or angular momentum transfer by control fields, or interactions with a reservoir in the environment. In particular various studies on quantum dots containing a single electron have shown that such DNP can indeed reduce the nuclear spin fluctuations [37, 35].

As further discussed in Chapter 4 of this thesis, we investigated the interaction between EIT driving and the occurrence of DNP, with the prospect to suppress the nuclear spin fluctuations via DNP by using EIT itself [38, 39]. As a first step, we used the EIT control-lasers to create a small nuclear spin polarization via DNP, and also used EIT as a probe for to studying the effect of it on the D^0 spin splitting, in a time-resolved manner.

1.6 Localized quantum systems in solids

Besides the D^0 system in GaAs, several other atom-like or molecule-like systems in solids (often with long-lived spin states) are currently investigated for quantum-information applications. In this section we will shortly review the most significant material systems and developments, and compare the properties to the D^0 system in GaAs. We restrict the discussion to optically-active quantum systems in solids.

1.6.1 Quantum dots

Optical manipulation of the spin states of single-electron and single-hole [40] systems has been widely studied already with single quantum dots, or ensembles of quantum dots [41]. A good example and important result is EIT-type control with a single quantum dot, that contained one electron [37]. These systems are mostly realized with III-V semiconductors, by growing small islands of III-V material with a lower band gap inside a host material with a higher band gap, such that charge carriers can be localized in the dots, and optical control is possible. The most widely studied example is InAs dots in a GaAs host. Since all stable isotopes that can form III-V semiconductors have non-zero nuclear spin, also in these systems the spins of localized charge carriers always have significant interaction with the ensemble of nuclear spins in the dot material. This implies that hyperfine interactions also contribute to limiting the electronic spin coherence time for III-V dots [37, 42, 35].

As compared to the D^0 system, the system-to-system variation due to limited control during quantum-dot growth is much larger (no control at the atomic scale), typically by a factor 10^5. Also, there are no clear technological prospects to improve on this. Consequently, state-of-the-art results on quantum-communication functionalities were mostly performed with a single quantum dot per functional qubit, and often required delicate tuning of the energy levels when working with more than one dot, or a dot coupled to a particular optical frequency [43, 44, 45, 46]. Still, despite these non-ideal aspects, III-V quantum dots have been studied extensively for quantum applications, since they were among the first material systems available for proof-of-principle studies. This led to demonstrations of various quantum-optical phenomena such as indistinguishable photons, photon bunching, and quantum entanglement between optical pulses and spins in quantum dots [21, 35, 47, 48, 49, 50, 51, 52, 53, 54, 55, 56].

1.6.2 Color centers in diamond and silicon carbide

A system that has been widely and very successfully studied as a qubit since 2003 is the nitrogen-vacancy (NV) center in diamond [11, 57, 58]. Driven by its favorable qubit properties, the material and device technology for diamond has been showing a very rapid development in this period as well. This system has very favorable properties: they can be studied as single centers, the optical emission is bright, and it has millisecond spin coherence times (spin echo) up to room temperature. In addition, with NMR and ESR control, advanced quantum

processing with electron-to-nuclear spin-state transfer has been demonstrated. It is a deep defect, and its electronic states are much more localized, roughly at the atomic scale. This also gives less favorable properties. The energy levels show stronger inhomogeneity from local strain variations in the material than the GaAs D^0 system. Further, upon optical emission, more than 95% is emitted via a phonon side band. Still, for solid-state qubits, the NV center has shown the most advanced performance, with as state of the art in 2015 a loop-hole free test of Bell inequalities [59] (advanced test of quantum entanglement with two spins widely separated in space).

More recently, a few other color centers with properties similar to the NV center were identified [60]. An interesting example is the divacancy in the wide-band-gap semiconductor SiC. This system also shows millisecond spin coherence times (spin echo) at room temperature, it has its optical transitions near telecom wavelength, and semiconductor device technology is already well developed for SiC [61]. EIT with a SiC divacancy ensemble was recently demonstrated [62].

1.6.3 Rare-earth doped crystals

Another interesting class of materials with quantum emitters are rare-earth doped crystals. Here, hyperfine levels can be spectrally resolved, giving access to direct optical control of the nuclear spin of the defect, which can show coherence times in excess of seconds. The optical transitions are weak, but also have a long coherence time. Strong inhomogeneous broadening of the optical transition is typical, but this can be remedied via long-lived spectral hole burning. While material and device technology are here not strongly developed, these systems have shown record performance for optical quantum memories, [14, 63, 64, 65], and very recently the first quantum-optical device structures were reported [66].

1.6.4 D^0 centers in silicon

Shallow D^0 donor systems also occur in silicon. The fact that silicon has an indirect band gap strongly compromises optical control. Despite this limitation, research with the Si D^0 system has shown record values for control of spin coherence, since bulk Si material can be isotopically enriched to a form where (nearly) all Si atoms having nuclear spin zero. Such materials can thus be used for studies of long electron spin coherence that is not compromised by hyperfine interactions. Even more interesting is that the D^0 electron then only has hyperfine interaction with a single nuclear spin: that of the D^0 core ion itself. An experiment on such a

D^0 ensemble that combined optical control, electron-nuclear spin-state transfer, and controlled D^0 ionization, showed a nuclear spin coherence time of 39 minutes at room temperature [67] (obtained while applying NMR spin-echo corrections).

1.6.5 D^0 centers in II-VI semiconductors

More recently, the D^0 systems in II-VI semiconductors were also investigated as a potential qubit (see for example Ref. [68] on ZnSe). The II-VI semiconductors have typically good optical properties (direct band gap), but with a band gap that is higher than GaAs. Here material technology is not as well developed as for GaAs. An interesting aspect of II-VI semiconductors is that some isotopes of the basic elements have nuclear spin zero. As for silicon, with isotopic enrichment this gives access to studies where hyperfine interactions do not limit electron spin coherence.

1.6.6 The D^0 system in GaAs: its contributions to the field

Before and in parallel with this PhD research, several other groups worked on the D^0 system in GaAs, and their results were of great value for this PhD research. Key examples since 2005 are CPT with D^0 ensembles [27, 28], pulsed optical control of spin states [69, 70, 36], and spin-noise spectroscopy [71].

Research on the D^0 system in GaAs has relevance for the entire field reviewed in this section. Arguably, a comparison with the other systems presented here indicates that it is not very likely that the GaAs D^0 system will come forward as the best platform for quantum applications. Still, besides some weak points, it also has some strong points. It is unique in combining strong optical transitions with a high degree of ensemble homogeneity in state-of-the-art materials. This makes it currently still one of the best systems for investigating EIT physics in solid-state material, while any limitations in EIT can be linked to solid-state properties that are (relative to other available materials) well understood and well controlled.

References

[1] M. A.Nielsen and I. L. Chuang, *Quantum Computation and Quantum Information* (Cambridge University Press, 2000).

[2] N. D. Mermin, *Quantum Computer Science* (Cambridge University Press, 2007).

[3] For a review of recent developments see: K. Southwell *et al.*, *Quantum coherence - Nature insight*, Nature **453**, 1003 (2008).

[4] For a review of recent developments see: T. D. Ladd *et al.*, *Quantum computers*, Nature **464**, 45 (2010).

[5] For a review of recent developments see: J. Stajic *et al.*, *The Future of Quantum Information Processing*, Science **339**, 1163 (2013).

[6] C. H. Bennett and G. Brassard, *Quantum cryptography: Public key distribution and coin tossing*, Proceedings of IEEE International Conference on Computers, Systems and Signal Processing **175**, 8 (1984).

[7] N. Gisin, G. Ribordy, W. Tittel, and H. Zbinden, *Quantum cryptography*, Rev. Mod. Phys. **74**, 145 (2002).

[8] P. W. Shor, *Polynomial-time algorithms for prime factorization and discrete logarithms on a quantum computer*, SIAM J. Comput. **26**, 1484 (1997).

[9] L. K. Grover, *Quantum Mechanics Helps in Searching for a Needle in a Haystack*, Phys. Rev. Lett. **79**, 325 (1997).

[10] D. D. Awschalom, N. Samarath, and D. Loss (eds.), *Semiconductor Spintronics and Quantum Computation* (Springer, Heidelberg, 2002).

[11] R. Hanson and D. D. Awschalom, *Coherent manipulation of single spins in semiconductors*, Nature **453**, 1043 (2008).

[12] L. M. Duan, M. D. Lukin, J. I. Cirac, and P. Zoller, *Long-distance quantum communication with atomic ensembles and linear optics*, Nature **414**, 413 (2001).

[13] H. J. Kimble, *The quantum internet*, Nature **453**, 1023 (2008).

[14] C. Simon *et al.*, *Quantum memories: A review based on the European integrated project "Qubit Applications (QAP)"*, Eur. J. Phys. D **58**, 1 (2010).

[15] T. E. Northup and R. Blatt, *Quantum information transfer using photons*, Nature Photonics **8**, 356 (2014).

[16] M. D. Lukin and A. Imamoglu, *Controlling photons using electromagnetically induced transparency*, Nature **413**, 273 (2001).

[17] M. D. Lukin, *Colloquium: Trapping and manipulating photon states in atomic ensembles*, Rev. Mod. Phys. **75**, 457 (2003).

[18] M. Fleischhauer, A. Imamoglu, and J. Marangos, *Electromagnetically induced transparency: Optics in coherent media*, Rev. Mod. Phys. **77**, 633 (2005).

[19] M. Mücke *et al.*, *Electromagnetically induced transparency with single atoms in a cavity*, Nature **465**, 755 (2010).

[20] J. McKeever *et al.*, *Deterministic generation of single photons from one atom trapped in a cavity*, Science **303**, 1992 (2004).

[21] K. Hennessy *et al.*, *Quantum nature of a strongly coupled single quantum dot-cavity system*, Nature **445**, 896 (2007).

[22] M. Cardona and P. Y. Yu, *Fundamentals of Semiconductors* (Springer-Verlag, 2001).

[23] M. Fox, *Optical Properties of Solids* (2^{nd} edition, Oxford University Press, 2010).

[24] F. Meier and B. P. Zakharchenya (eds.), *Optical orientation* (Elsevier, Amsterdam, 1984).

[25] J. M. Kikkawa and D. D. Awschalom, *Resonant Spin Amplification in n-Type GaAs*, Phys. Rev. Lett. **80**, 4313 (1998).

[26] V. A. Karasyuk, D. G. S. Beckett, M. K. Nissen, A. Villemaire, T. W. Steiner, and M. L. W. Thewalt, *Fourier-transform magnetophotoluminescence spectroscopy of donor-bound excitons in GaAs*, Phys. Rev. B **49**, 16381 (1994).

[27] K.-M. Fu, C. Santori, C. Stanley, M. Holland, and Y. Yamamoto, *Coherent Population Trapping of Electron Spins in a High-Purity n-Type GaAs Semiconductor*, Phys. Rev. Lett. **95**, 187405 (2005).

[28] T. Wang, R. Rajapakse, and S. F. Yelin, *Electromagnetically induced transparency and slow light with semiconductor bound excitons*, Optics Comm. **272**, 154 (2007).

[29] C. W. Chou *et al.*, *Measurement-induced entanglement for excitation stored in remote atomic ensembles*, Nature **438**, 828 (2005).

[30] D. N. Matsukevich *et al.*, *Entanglement of Remote Atomic Qubits*, Phys. Rev. Lett. **96**, 030405 (2006).

[31] L. V. Hau *et al.*, *Light speed reduction to 17 metres per second in an ultracold atomic gas*, Nature **397**, 594 (1999).

[32] D. F. Phillips *et al.*, *Storage of Light in Atomic Vapor*, Phys. Rev. Lett. **86**, 783 (2001).

[33] C. H. van der Wal and M. Sladkov, *Towards quantum optics and entanglement with electron spin ensembles in semiconductors*, Solid State Sci. **11**, 935 (2009).

[34] A. Abragam, *The Principles of Nuclear Magnetism* (Oxford University Press, 1961).

[35] B. Urbaszek *et al.*, *Nuclear spin physics in quantum dots: An optical investigation*, Rev. Mod. Phys. **85**, 79 (2013).

[36] S. M. Clark, K.-M. C. Fu, Q. Zhang, T. D. Ladd, C. Stanley, and Y. Yamamoto, *Ultrafast optical spin echo for electron spins in semiconductors*, Phys. Rev. Lett. **102**, 247601 (2009).

[37] X. Xu *et al.*, *Optically controlled locking of the nuclear field via coherent dark-state spectroscopy*, Nature **459**, 1105 (2009).

[38] A. R. Onur, *Optical control of mesoscopic spin ensembles in gallium arsenide* (PhD thesis, University of Groningen, 2015).

[39] J. P. de Jong, *Optically addressing semiconductor electron-spin ensembles with tunable nuclear-spin environments* (PhD thesis, University of Groningen, 2016).

[40] D. Brunner *et al.*, *A coherent single-hole spin in a semiconductor*, Science **325**, 70 (2009).

[41] R. J. Warburton, *Single spins in self-assembled quantum dots*, Nature Materials **12**, 483 (2013).

[42] C. Latta *et al.*, *Confluence of resonant laser excitation and bidirectional quantum-dot nuclear-spin polarization*, Nature Physics **5**, 758 (2009).

[43] M. T. Rakher *et al.*, *Externally Mode-Matched Cavity Quantum Electrodynamics with Charge-Tunable Quantum Dots*, Phys. Rev. Lett. **102**, 097403 (2009).

[44] R. B. Patel *et al.*, *Two-photon interference of the emission from electrically tunable remote quantum dots*, Nature Photonics **4**, 632 (2010).

[45] J. Gudat *et al.*, *Permanent tuning of quantum dot transitions to degenerate microcavity resonances*, Appl. Phys. Lett. **98**, 121111 (2011).

[46] J. H. Prechtel *et al.*, *Frequency-stabilized source of single photons from a solid-state qubit*, Phys. Rev. X **3**, 041006 (2013).

[47] C. Santori *et al.*, *Indistinguishable photons from a single-photon device*, Nature **419**, 594 (2002).

[48] S. Strauf *et al.*, *High-frequency single-photon source with polarization control*, Nature Photonics **1**, 704 (2007).

[49] J. Berezovsky *et al.*, *Picosecond coherent optical manipulation of a single electron spin in a quantum dot*, Science **320**, 349 (2008).

[50] D. Press, T. D. Ladd, B. Zhang, and Y. Yamamoto, *Complete quantum control of a single quantum dot spin using ultrafast optical pulses*, Nature **456**, 218 (2008).

[51] E. B. Flagg *et al.*, *Interference of Single Photons from Two Separate Semiconductor Quantum Dots*, Phys. Rev. Lett. **104**, 137401 (2010).

[52] A. N. Vamivakas *et al.*, *Observation of spin-dependent quantum jumps via quantum dot resonance fluorescence*, Nature **467**, 297 (2010).

[53] K. De Greve *et al.*, *Quantum-dot spin-photon entanglement via frequency downconversion to telecom wavelength*, Nature **491**, 421 (2012).

[54] Y.-M. He *et al.*, *On-demand semiconductor single-photon source with near-unity indistinguishability*, Nature Nano. **8**, 213 (2013).

[55] A. V. Kuhlmann *et al.*, *Transform-limited single photons from a single quantum dot*, Nature Comm. **6**, 8204 (2015).

[56] A. Delteil *et al.*, *Generation of heralded entanglement between distant hole spins*, Nature Physics **12**, 218 (2016).

[57] C. Santori *et al.*, *Coherent Population Trapping of Single Spins in Diamond under Optical Excitation*, Phys. Rev. Lett. **97**, 247401 (2006).

[58] V. V. Dobrovitski *et al.*, *Quantum Control over Single Spins in Diamond*, Annual Review of Condensed Matter Physics **4**, 23 (2013).

[59] B. Hensen *et al.*, *Loophole-free Bell inequality violation using electron spins separated by 1.3 kilometres*, Nature **526**, 682 (2015).

[60] J. R. Weber *et al.*, *Quantum Computing with Defects*, Proc. Nat. Acad. Sci. **107**, 8513 (2010).

[61] W. F. Koehl *et al.*, *Room temperature coherent control of defect spin qubits in silicon carbide*, Nature **479**, 84 (2011).

[62] O. V. Zwier, *Two-laser spectroscopy and coherent manipulation of color-center spin ensembles in silicon carbide* (PhD thesis, University of Groningen, 2016).

[63] J. J. Longdell, *et al.*, *Stopped light with storage times greater than one second using electromagnetically induced transparency in a solid*, Phys. Rev. Lett. **95**, 063601 (2005).

[64] M. P. Hedges *et al.*, *Efficient quantum memory for light*, Nature **465**, 1052 (2010).

[65] Georg Heinze, Christian Hubrich, and Thomas Halfmann, *Stopped Light and Image Storage by Electromagnetically Induced Transparency up to the Regime of One Minute*, Phys. Rev. Lett. **111**, 033601 (2013).

[66] D. Ding *et al.*, *Multidimensional Purcell effect in an ytterbium-doped ring resonator*, Nature Photonics **10**, 385 (2016).

[67] K. Saeedi *et al.*, *Room-Temperature Quantum Bit Storage Exceeding 39 Minutes Using Ionized Donors in Silicon-28*, Science **342**, 830 (2013).

[68] T. D. Ladd *et al.*, *Fluorine-doped ZnSe for applications in quantum information processing*, Phys. Stat. Sol. B **246**, 1543 (2010).

[69] K.-M. C. Fu *et al.*, *Millisecond spin-flip times of donor-bound electrons in GaAs*, Phys. Rev. B **74**, 121304 (2006).

[70] K.-M. C. Fu *et al.*, *Ultrafast control of donor-bound electron spins with single detuned optical pulses*, Nature Physics **4**, 780 (2008).

[71] F. Berski *et al.*, *Interplay of Electron and Nuclear Spin Noise in n-Type GaAs*, Phys. Rev. Lett. **115**, 176601 (2015).